

NEAR INFRARED FILTER MANUFACTURING SPECIFICATIONS FOR GEMINI INSTRUMENTS

DOUG SIMONS
AUGUST 1996

1.0 Purpose

This technical note is supplemental to TN-PS-G0037 titled "Near Infrared Filter Bandpasses For Gemini Instruments" and provides manufacturing specifications for the near-infrared filters to be used in Gemini's instrumentation. Manufacturing specifications for the proposed filters are listed and in most cases the filters proposed match those already in regular use at numerous observatories. The most significant departure from existing standards is the proposed J-band filter, which attempts to correct for fairly large mismatches in J-band filters with the atmospheric transmission in this spectral region.

2.0 Filter Specifications

Figure 1 illustrates the parameters used to define filter bandpass. The width specification ($\Delta\lambda$) is tied to 50% of the peak transmittance. Roll-off is defined as the change in wavelength between 10% and 90% of the peak transmission. The filter operating range is the wavelength range in which the blocking specification applies, except of course where the desired transparent bandpass falls.

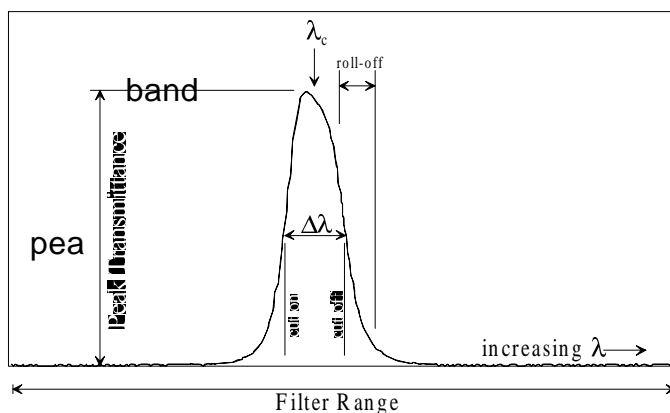


Figure 1 - Basic filter definition parameters are graphically represented. See the text in sections 2 and 3 for explanations.

- Filter operating range 0.4 - 6.0 μm (VISMIR/InSb detector compatible)
- Out of band transmission $<10^{-4}$ (blocking for InSb separate). Option for separate PK50 blocker vs. built-in blocker for each filter available
- Bandwidth specifications are listed in Table 1 for both broadband and commonly used narrowband filters. Note that all narrowband filters have a $\Delta\lambda = 1\%$ bandpass unless otherwise specified
- All parameters specified for 77 °K and 77 °K scans provided for each batch across the entire filter operating range

- >50% peak transmission (goal >60%) for narrowband filters

- >80% peak transmission (goal >90%) for broadband filters

- Cut-on tolerance -0.00, +0.01 μm for broadband filters, ± 0.002 μm for narrowband filters

- Cut-off tolerance -0.01, +0.00 μm for broadband filters, ± 0.002 μm for narrowband filters

- Roll-off tolerance: rise from 10-90% peak transmission in <0.04 μm for broadband filters, <0.005 μm for narrowband filters

- Peak transmission level to $\pm 5\%$ across broadband filters

- Substrate flatness <30 nm rms (compatible with AO systems)

- Maximum thickness 5 mm, including Pk50 blocker

- 60 mm diameter with option for other diameters upon request

- Free of pinhole defects

Filter Name	Cut-on Wavelength (μm)	Cut-off Wavelength (μm)
Broadband		
J	1.17	1.33
H	1.49	1.78
K'	1.95	2.29
K _s	1.99	2.31
K	2.03	2.37
K _l	2.07	2.41
L'	3.42	4.12
M'	4.57	4.79
Narrowband		
Z	0.996	1.069
He I	1.078	1.088
Pa γ	1.089	1.099
O II	1.231	1.243
J continuum	1.251	1.263
Pa β	1.276	1.288
H continuum	1.560	1.580
[Fe II]	1.636	1.652
H ₂ v=1-0 S(1)	2.111	2.133
Br γ	2.155	2.177
H ₂ v=2-1 S(1)	2.237	2.259
K continuum	2.260	2.280
CO(2-0) band head	2.284	2.306
CO(3-1) band head	2.312	2.336
CO(4-2) band head	2.342	2.366
H ₂ O Ice	3.085	3.115
PAH	3.250	3.305
Br α continuum	3.964	4.016
Br α	4.032	4.072

Table 1 - Bandpasses for both broadband and narrowband filters are listed. All of the broad band filters listed above are discussed in the accompanying technical note, TN-PS-G0037. The proposed list of narrowband filters is patterned from the consortium organized by Mike Skrutskie in 1992.

3.0 Rationale for Specifications

Careful consideration needs to be given to several key design aspects of the proposed filter set. Since a consortium of buyers is expected, arriving at a single set of

parameters that are tuned to meet end-users is difficult, but a reasonable set of fabrication constraints can be determined, guided by modern thin film technology, the atmospheric models described in the accompanying technical note, and general instrumentation principles. Accordingly this section discusses requirements on tip angle, operating temperature, optical quality, roll-off, and band-edge tolerances for the filters.

3.1 Angle of Incidence

The following equation describes the shift of shorter wavelengths that the operating bandpass of a filter suffers as it is tipped with respect to the angle of incidence of an optical system.

$$\lambda_{\theta} = \lambda_0 \frac{(n^2 - \sin^2 \theta)^{1/2}}{n} \quad (1)$$

Here, λ_{θ} is the central wavelength at the angle of incidence θ , λ_0 is the central wavelength at $\theta = 0$, and n is the effective refractive index of the filter. For the broadband filter bandpasses listed in Table 1, Figure 2 shows the shift in λ_c as a function of angle of incidence assuming an effective refractive index of 1.4. Since the shift to shorter wavelengths drops with increasing index, and most materials (thin films and substrates) have indices that do not fall below ~ 1.4 , this essentially represents a worst case set of λ_c shifts. Typically filters are tipped in instruments when very low or collimated beams are used in order to reduce internal reflections. The exact amount of tip is instrument specific hence pinning λ_c to a specific tip angle is not possible in a consortium of filter users. Instead the filters are specified on the assumption that $\theta = 0$ and users who wish to tip filters should consult Figure 2 to determine if the shift in bandpass is important. For a common tip angle of 5° the worst case amounts to $<0.01 \mu\text{m}$ for the M' filter. For the J, H, and K filters the shift is $<0.005 \mu\text{m}$.

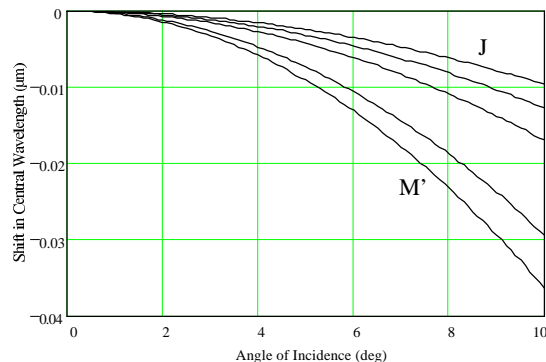


Figure 2- Equation 1 is used to plot the shift of shorter wavelengths of λ_c for the broadband filters proposed as a function of angle of incidence.

3.2 Temperature Dependence

Just as instruments will use filters at various tip angles, they will also use them at various temperatures. Typically instruments using so-called nonthermal detectors (e.g., Hg: Cd: Te), operating at wavelengths under $\sim 2.5 \mu\text{m}$, run at $\sim 77^\circ\text{K}$ while InSb based instruments run substantially colder (e.g. $\sim 40^\circ\text{K}$). Temperature dependencies in interference filters are due to changes in refractive index (Δn) and mechanical

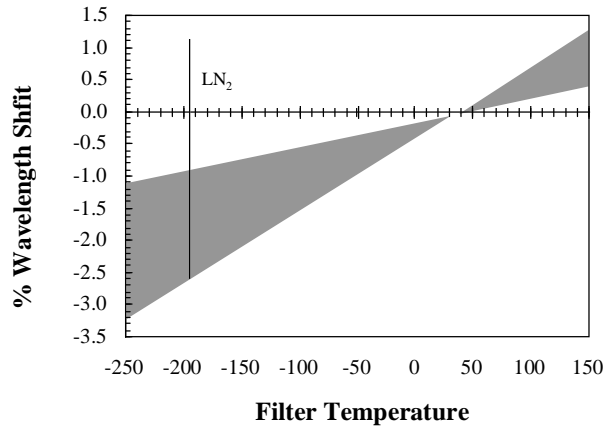


Figure 3 - For a filter designed to nominally operate at room temperature, the change in λ_c as a function of temperature is shown as a shaded region. This is adopted from The Infrared Handbook (1978, ed. Wolfe & Zissis) and illustrates the typical range in substrates and films used in interference filters.

thickness (t_g) in the interfering layers as they are cooled. Equation 2 shows how these parameters also change with temperature, ΔT .

$$\frac{\Delta n t_g}{\Delta T} = n \frac{\Delta t_g}{\Delta T} + t_g \frac{\Delta n}{\Delta T} \quad (2)$$

A range of substrate and thin film materials might be used to fabricate a filter set and some of this information is no doubt proprietary to manufacturers, hence quantifying temperature effects in detail is difficult and only a range of likely values can be considered. Since the parameters in equation 2 to first order depend linearly with temperature, the change in a filter's bandpass with temperature is essentially linear. As seen in Figure 3, typically filters change by ~2% in λ_c when cooled from room temperature to 77 °K. This is a highly predictable parameter in the design of a filter but, given that the sample Bry filter shown in Figure 4 only experiences a ~0.7% shift in central wavelength, the range depicted in Figure 4 should really only be taken as illustrative of the effect. As previously mentioned, it is expected that the proposed filters will be used in instruments working between 77 to ~40 °K, and over this range in temperature the shift in λ_c is expected to be typically a ~0.2%, since wavelength shifts vary linearly with temperature. This is comparable to the shift induced by tipping the filter by ~5°.

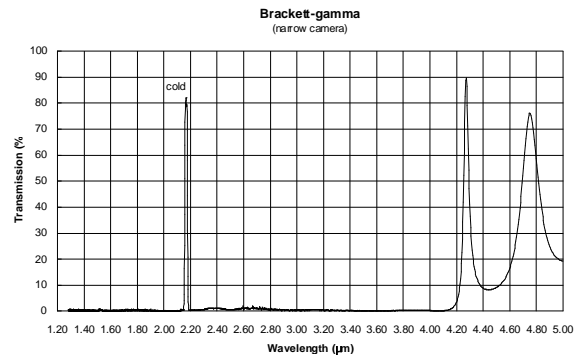
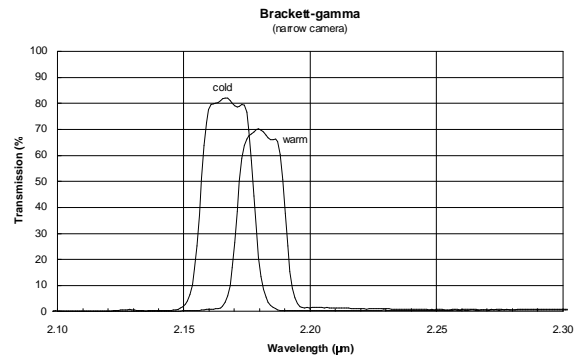


Figure 4 Cold scans of filters used in CFHT's "Redeye" cameras are shown to illustrate typical shifts in central wavelength between room temperature and °K. 77 Note that the peak transmittance also changes with temperature. The bottom plot shows the leaks in the filter, which are not an issue for Redeye (Hg: Cd: Te detector) but would lead to be locked for instruments with longer wavelength sensitivity.

3.3 Optical Surface Quality

With the future use of adaptive optics at various sites it is important to set the optical surface irregularity specification with high Strehl optical systems in mind. For Strehls greater than ~0.2 the relation,

$$\text{Strehl} \approx e^{-\left(\frac{2\pi\sigma}{\lambda}\right)^2} \quad (3)$$

can be used to estimate the Strehl degradation when a filter is placed in an otherwise perfect optical system. In this relation σ is the rms wavefront error induced by an optical element working at wavelength λ . Past filters have typically been specified in terms of peak-to-peak irregularities not exceeding $\lambda/4$ at HeNe (~0.6 μm). Assuming a typical AO application working as short as the H-band at 1.65 μm , the Strehl would be degraded by a factor of 0.94 with this specification, which is a significant fraction of the error budget in well designed, diffraction limited, imaging systems. The proposed specification of 30 nm rms error corresponds to $\lambda/8$ peak-to-peak irregularity at HeNe or a Strehl of 0.985 at H. Allocating ~1% Strehl degradation to filters in typical AO instrument error budgets is probably acceptable and pushing for flatter substrates is probably a cost driver in the filters, particularly the Pk50 blocking elements.

3.4 Bandwidth Tolerances

The aforementioned tolerances are tied to how the atmosphere absorbs in the regions immediately surrounding the proposed

broadband filters. Figure 5 shows the H-band filter with a Mauna Kea atmosphere at 1.0 and 1.3 airmasses. Changes in the edge windows are due to changes in water vapor or simply telescope pointing. As seen in Figure 5 a shift in the edge of the bandpass at the ~0.01 μm level is significant compared to the sharpness of the edge of the atmospheric window. This implies that bandwidth tolerances for broadband filters should be held to no worse than the same ~0.01 μm level to assure that the filters are not prone to contributing significant photometric errors during typical observations

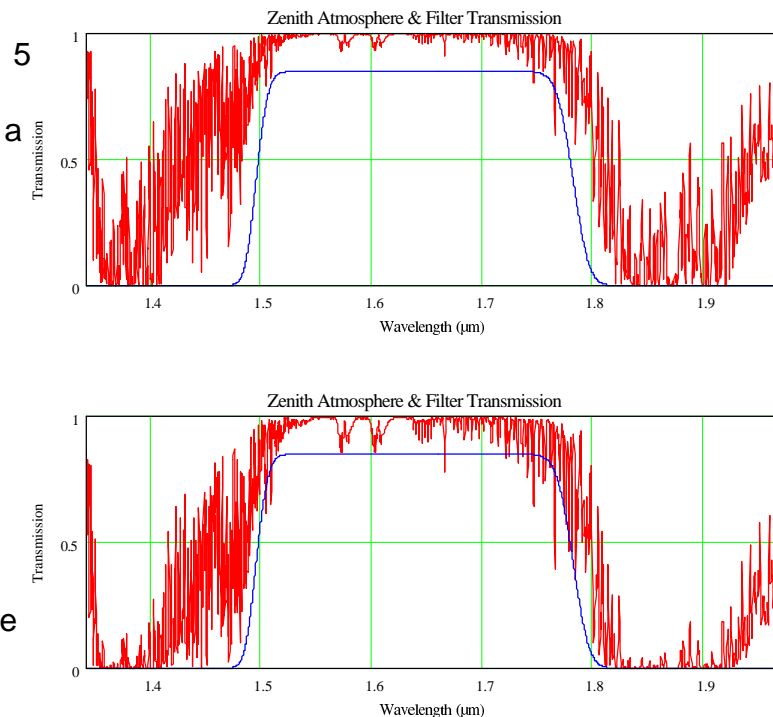


Figure 5- The proposed H-band filter is shown together with the Mauna Kea atmosphere (1 mm PWV) for 1.0 and 1.3 airmasses. Note where the spectral region immediately surrounding the proposed bandpass fills in with changing air mass and/or atmospheric water vapor.

spanning ~1-3 airmasses. The accompanying technical note shows that the change in photometric error contribution with a ~0.01 μm change in $\Delta\lambda$ is ~0.1 millimag for the H-band filter. This is certainly small compared to other error sources in typical near-infrared photometry applications. Also, given equations 1 and 2 and figures 2 and 3, there will be a range in bandpasses for the same set of filters used in different instruments. Crudely estimated, these error sources rss'd together yield $\sim(.01^2 + 0.003^2 + .003^2)^{1/2} \sim .011 \mu\text{m}$ shifts in bandpass centers and edges across various instruments, using the proposed manufacturing specifications. Given the modeling results in TN-PS-G0037, this small level of bandpass shift between filters in different instruments should lend to the photometric transformations between sites than ~~sp~~a filters have supported, with no loss in sensitivity.